



## 1 Abstract

Stellar activity hinders the detection of small exoplanets with the radial velocity (RV) method, because it introduces spurious signals that can drown or mimic planetary signatures (Queloz et al. 2001, Huelamo et al. 2008). It is therefore crucial to understand and filter out activity signals, especially in light of future small planet searches.

We investigate ways to reduce activity jitter in RV time series using spectropolarimetric data sets in optical (ESPaDONs@CHFT and NARVAL@TBL), and in near-infrared (nIR) with SPIROU@CHFT. We employ two approaches: 1) perform a chromatic study of typical stellar activity proxies, 2) study a parametric selection of spectral lines to build a mask for Least-Square Deconvolution (Donati et al. 1997). The study is performed for EV Lac and AD Leo, two very active M dwarfs.

## 2 Period analysis

Typical activity-filtering procedures inspect the periodic variability of known activity indicators and the RV data sets to find a correlation.

Examples of indicators are the FWHM and line bisector (B<sub>l</sub>, Queloz et al. 2001, Boisse et al. 2009), or the longitudinal magnetic field of the star (B<sub>l</sub>, Donati et al. 1997, Hebrard et al. 2016).

We use datasets from years with the largest number of observations, detrend long-term variations with a quadratic fit and apply the Generalized Lomb-Scargle (GLS, Fig. 1) periodogram (Zechmeister & Kürster 2009).

For both EV Lac and AD Leo, the optical RV data feature a significant peak at the stellar rotation period, but not in nIR (Table 1). B<sub>l</sub> yields the expected stellar rotation period in all cases.

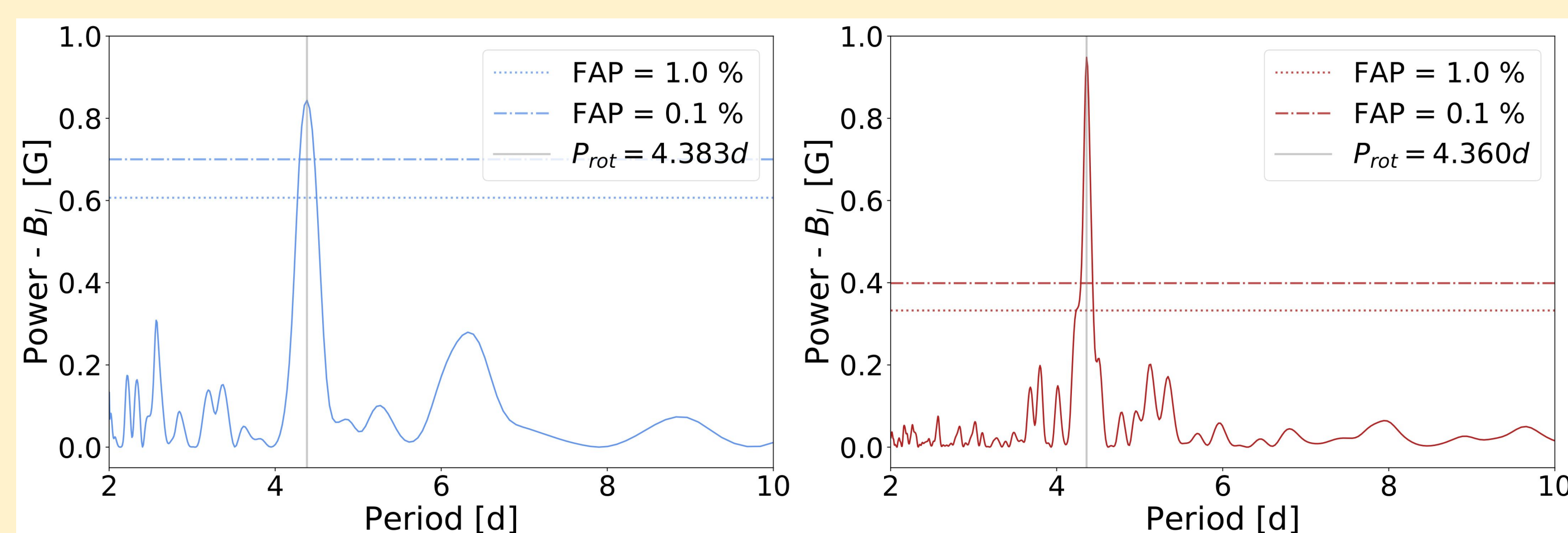


Fig. 1. Generalized Lomb-Scargle periodogram of the longitudinal magnetic field of EV Lac for 2010 in optical (left) and 2020 in nIR (right).

## 3 Parametric selection of line masks

We select subsets of an atomic (in optical) or molecular (in nIR) line mask by splitting it according to thresholds of line parameters: wavelength, magnetic sensitivity and depth.

We obtain the corresponding RV data sets and 3- $\sigma$  clip them to clean from outliers.

We record the radial velocity semi-amplitude (K) of the resulting data set to find the mask that mitigates the activity signal the most (Fig. 2).

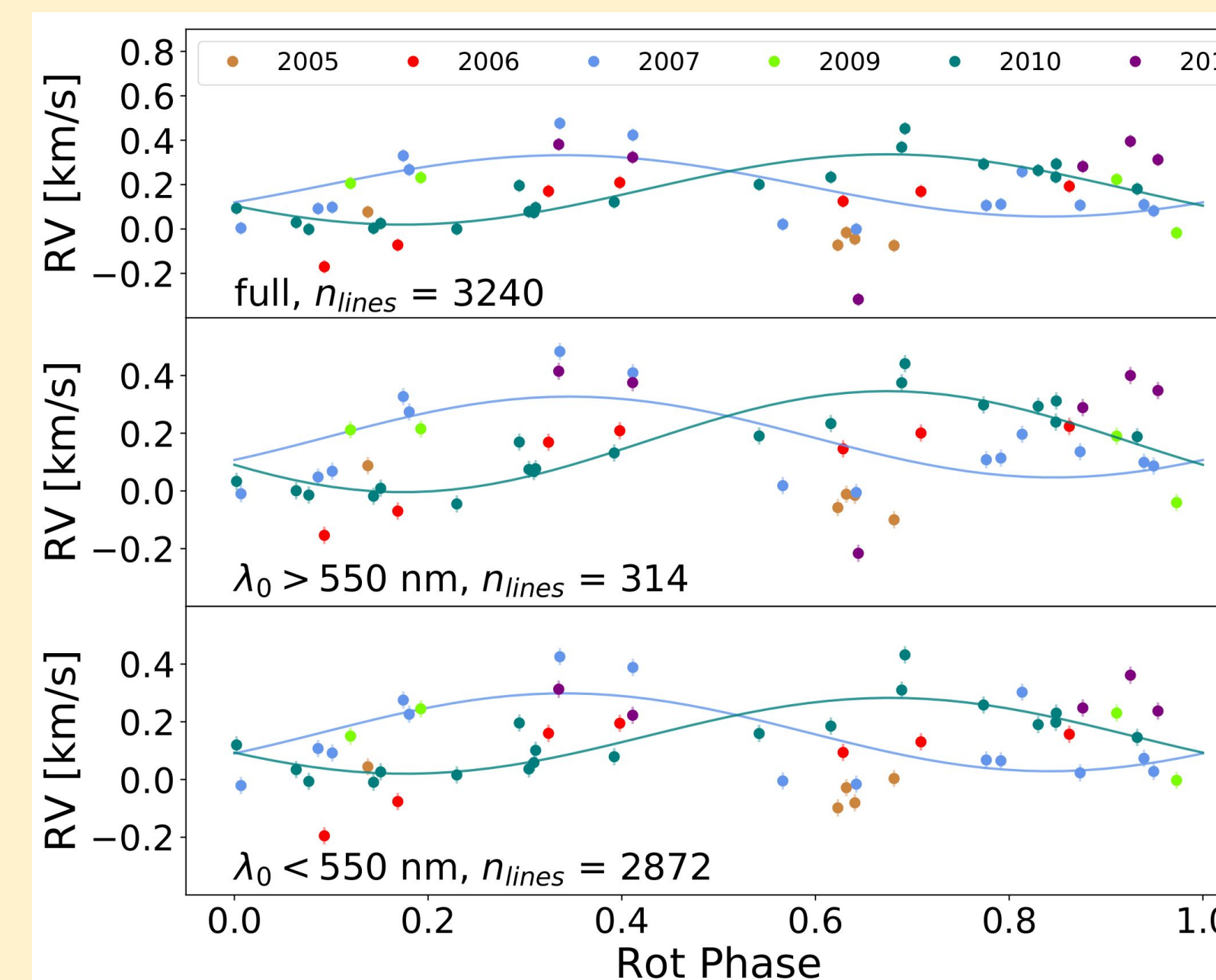


Fig. 2. Phase-fold RV data set obtained with the full mask and the  $\lambda$ -selected ones for EV Lac in optical. Sinusoidal fits of the densest years are shown.

| EV Lac         |           |           |               |           |
|----------------|-----------|-----------|---------------|-----------|
|                | Optical   |           | near-Infrared |           |
| Quantity       | 2010      | 2007-2010 | 2020          | 2019-2020 |
| RV             | 4.351 d   | 4.412 d   | 2.184 d       | /         |
| B <sub>l</sub> | 4.351 d   | 4.335 d   | 4.360 d       | 4.361 d   |
| FWHM           | 4.351 d   | 4.345 d   | 4.348 d       | 4.365 d   |
| BIS            | 4.415 d** | 4.450 d** | 2.662 d*      | /         |
| AD Leo         |           |           |               |           |
|                | Optical   |           | near-Infrared |           |
| Quantity       | 2008      | 2007-2008 | 2020          | 2019-2020 |
| RV             | 2.216 d** | 2.200 d   | /             | /         |
| B <sub>l</sub> | 2.234 d   | 2.239 d   | 2.232 d       | 2.230 d   |
| FWHM           | 2.269 d   | 2.272 d** | /             | /         |
| BIS            | 2.234 d   | 2.256 d   | 2.995 d*      | 2.308 d*  |

\* means FAP > 10%, \*\* means 1% < FAP < 10%, otherwise FAP < 0.1%

Table 1. Results of the period search. In some cases, the first harmonic of the expected stellar rotation period has a significant peak, while in others (denoted as '/') the retrieved peak is spurious due to, e.g., the cadence of the observing windows.

| EV Lac           |                |                        |                |                        |
|------------------|----------------|------------------------|----------------|------------------------|
|                  | Optical        |                        | near-Infrared  |                        |
| Parameter        | Line selection | K [m s <sup>-1</sup> ] | Line selection | K [m s <sup>-1</sup> ] |
| Full mask        | /              | 158                    | /              | 34                     |
| $\lambda$ [nm]   | >550, <550     | 175,131                | >1650, <1650   | 25, 43                 |
| g <sub>eff</sub> | >1.2, <1.2     | 157,152                | /              | /                      |
| depth            | >0.5,0.7,0.9   | 167,181,141            | >0.05, 0.1     | 33, 38                 |
| AD Leo           |                |                        |                |                        |
|                  | Optical        |                        | near-Infrared  |                        |
| Parameter        | Line selection | K [m s <sup>-1</sup> ] | Line selection | K [m s <sup>-1</sup> ] |
| Full mask        | /              | 49                     | /              | 6                      |
| $\lambda$ [nm]   | >550, <550     | 52, 58                 | >1650, <1650   | 2, 8                   |
| g <sub>eff</sub> | >1.2, <1.2     | 45, 38                 | /              | /                      |
| depth            | >0.5,0.7,0.9   | 51, 48, 40             | >0.05, 0.1     | 5, 6                   |

Table 2. Results of the parametric selection. Reported are the conditions with which the masks are selected, and the resulting RV semi-amplitude. We use observations from the densest years for both stars.

## 4 Conclusions

- B<sub>l</sub> is a reliable activity tracer as the stellar period is always retrieved consistently and its estimates are compatible regardless of the line selection.
- A parametric selection is not sufficient to build a sub-mask to mitigate activity.
- The robustness of activity indicators based on the Stokes I profile to find the stellar rotation period decreases when switching from optical to nIR domain.
- The chromatic nature of stellar activity will be used to improve the efficiency of modelling and filtering techniques such as Doppler Imaging, Zeeman-Doppler Imaging, Gaussian Processes (Donati et al. 2016, Hebrard et al. 2016, Haywood et al. 2014).

## 5 Bibliography

- Queloz et al. 2001, A&A, 379, 279-287
- Huelamo et al. 2008, A&A, 2, L9-L13
- Donati et al. 1997, MNRAS, 291, 658
- Boisse et al. 2009, A&A, 495, 959-966
- Donati et al. 2016, Nature, 7609, 662-666
- Hebrard et al. 2016, MNRAS, 461, 1465-1497
- Haywood et al. 2014, MNRAS, 443, 2517-2531
- Zechmeister & Kürster 2009, A&A, 496, 577-584